Wave Refraction and Wave Height Variation Due to Current

By Yuichi IWAGAKI, Tetsuo SAKAI,
Toshio TSUDA and Yukio OKA

(Manuscript received June 10, 1977)

Abstract

This paper deals with the wave refraction due to current by a theoretical treatment and a numerical model. The theory of refraction of deep-water waves traversing a simple horizontal current with vertical axis of shear by Longuet-Higgins and Stewart[1] is extended to the case of shallow-water waves. It is found that the wave direction and wave height of shallow-water waves refracted by the current vary more rapidly than those of deep-water waves, and the variation of wave height is expressed as the product of the similar coefficients to the shoaling and refraction coefficients and a coefficient representing the effect of the radiation stress. A numerical model is presented for the wave refraction due to current. The variation of wave direction is calculated with the wave orthogonal equation along a path propagating in the direction of the sum of the wave velocity and the current, which is derived from the irrotational condition of wave number. The variation of wave height is also calculated with the equation of wave energy conservation in current derived by Longuet-Higgins and Stewart[1] along another path propagating in the direction of the sum of the group velocity and the current. The numerical results agree roughly with the theoretical results, and the validity of the numerical model is roughly confirmed. The effects of the relative wave velocity to the current, the derivatives of wave direction with respect to the horizontal coordinates and the radiation stress on the wave refraction due to current are found to be not negligible.

1. Introduction

Refraction of waves due to current is one of wave transformation phenomena. This phenomenon has not been investigated so widely compared with wave shoaling, wave refraction by underwater topography and wave diffraction.

Longuet-Higgins and Stewart[1] presented a wave energy conservation equation in current including the so-called radiation stress. They showed that the existing theoretical treatments[2)~4)] for the wave height variation of the refracted waves due to current failed to take the effect of this radiation stress into account. Taking the radiation stress into account, they solved the deep-water wave refraction due to current in special cases theoretically. They neglected the effect of the waves on the current.

In this paper, a theoretical treatment of the shallow-water wave refraction due to current in the same case as Longuet-Higgins and Stewart treated is presented. These theoretical results, however, can predict the wave refraction due to current only in special cases. A numerical model is necessary for the prediction of the wave refraction due to current of arbitrary distribution.

Recently, several theoretical models for the prediction of nearshore circulations due to waves in the surf zone have been presented[5)-10)]. These theories neglected the wave-current interaction as the first step to predict the nearshore circulation. Noda, Sonu, Rupert and Collins[11)] and Skovgaard and Jonsson[12)] presented independently numerical models for the prediction of the wave-current interaction. Noda et al. made use of a kinematic conservation equation of waves in current by Phillips[3)] and the dynamic conservation equation of wave energy in current by Longuet-Higgins and Stewart[1)]. They repeated the computation of the current induced by the waves and the computation of the wave refraction due to the current alternately to take the effects of the wave-current interaction on the nearshore circulation into consideration. Skovgaard and Jonsson made use of a wave energy conservation equation of different type from that by Longuet-Higgins and Stewart which they called "the equation of wave action conservation".

A similar numerical model for prediction of wave refraction due to current is presented here. The same two equations as Noda et al. used are applied as the basic equations. The current, however, is assumed not to be affected by the waves in contrast to two models mentioned above. The wave direction is calculated by a technique of integrating along characteristic lines similar to the conventional numerical technique of the wave refraction by underwater topography[14)]. The wave height is also calculated by the technique of integrating along characteristic lines different from those mentioned above.

This numerical model is applied to special cases which are able to be predicted by the theoretical treatment. The numerical results are compared with the theoretical ones, and the validity of the numerical model is discussed. The effects of the relative wave celerity, the derivatives of wave direction and the radiation stress are also discussed with the numerical results.

2. Theoretical Treatment of Wave Refraction Due to Current

2.1 Deep-water wave refraction due to current[1)]

Longuet-Higgins and Stewart[1)] treated a case of waves traversing a simple horizontal current with vertical axis of shear. The stream velocity $(U, 0, 0)$ is supposed to be everywhere parallel to the x-axis and also

$$\partial U/\partial x=\partial U/\partial z=0, \tag{1}$$

The angle of the wave direction with the x-axis is denoted by θ (Fig. 1). It is assumed that the range of value of θ is $0^\circ\sim90^\circ$ and U takes both positive and negative values. The wave number k is irrotational due to the definition of the wave number (Phillips[13)]), that is,

$$\partial k_x/\partial y-\partial k_y/\partial x=0, \tag{2}$$

where k_x and k_y are the x- and y-components of $\boldsymbol{k}$. Since the current varies only in the y-direction, the wave length and wave height are independent of x. Furthermore,

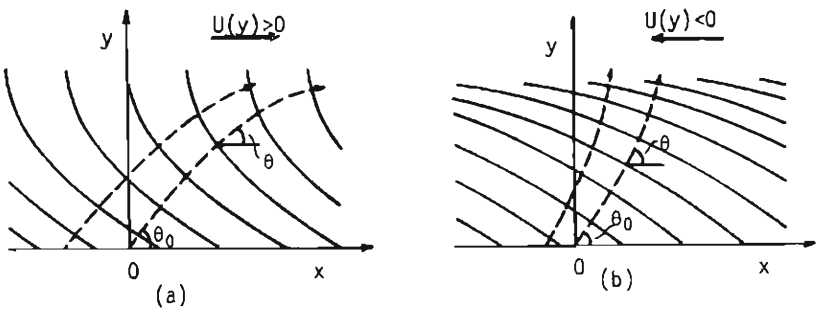

Fig. 1. Definition diagram for waves on a shearing current.

the wave number in the x-direction is $k \cos\theta$. So, we have

$$k \cdot \cos\theta = \text{const.} = b, \tag{3}$$

The kinematic conservation equation for the wave number given by Phillips is as follows:

$$\partial \boldsymbol{k}/\partial t + \nabla\omega = 0, \tag{4}$$

where ω is the apparent angular frequency of the waves relative to a fixed point. Since the apparent velocity of the waves at right-angles normal to their crests is $(c_* + U\cos\theta)$ and their wave number is k, the apparent angular frequency ω of the waves is $k\,(c_* + U\cos\theta)$. Therefore, considering the steady state, equation (4) becomes

$$k(c_* + U\cos\theta) = \sigma_0, \tag{5}$$

where c_* is the relative wave velocity to the current in the presence of current and σ_0 the angular frequency of the waves in the region of no current. Thirdly, we have the relation connecting the local wave number and the relative wave velocity in deep-water waves:

$$k \cdot c_*^2 = g. \tag{6}$$

Equation (6) is applicable if the water depth and the current vary slowly. From equations (3), (5) and (6), we have

$$c_*/c_0 = 1/(1 - U/c_0 \cdot \cos\theta_0), \tag{7}$$

$$k/k_0 = (1 - U/c_0 \cdot \cos\theta_0)^2, \tag{8}$$

$$\cos\theta/\cos\theta_0 = 1/(1 - U/c_0 \cdot \cos\theta_0)^2, \tag{9}$$

where c_0, k_0 and θ_0 denote the values of c, k and θ in the region of no current. It should be noticed that in general c_0, k_0 and θ_0 are not the values in deep water but in this case they are equal to the values in deep water.

The refracted wave height variation in the current is calculated by using the wave energy conservation equation in current[1]:

$$\partial E/\partial t+\partial\{E(U+c_{g*x})\}/\partial x+\partial\{E(V+c_{g*y})\}/\partial y$$
$$+S_{xx}\cdot\partial U/\partial x+S_{xy}\cdot\partial V/\partial x+S_{yx}\cdot\partial U/\partial y+S_{yy}\cdot\partial V/\partial y=0. \tag{10}$$

S is the so-called radiation stress and given as follows:

$$S=E\begin{Bmatrix}\frac{c_{g*}}{c_*}\cos^2\theta+\frac{1}{2}\left(\frac{2c_{g*}}{c_*}-1\right), & \frac{c_{g*}}{c_*}\cos\theta\cdot\sin\theta\\ \frac{c_{g*}}{c_*}\cos\theta\cdot\sin\theta, & \frac{c_{g*}}{c_*}\sin^2\theta+\frac{1}{2}\left(\frac{2c_{g*}}{c_*}-1\right)\end{Bmatrix}, \tag{11}$$

where c_{g*} is the relative group velocity of the waves to the current, c_{g*x} and c_{g*y} the x- and y-components of c_{g*} and E the wave energy. Johnson[3] considered the same case without taking into account the radiation stress. The group velocity in deep water is given by $1/2\cdot c_*$. Hence equation (10) becomes in the steady state, eliminating all derivatives with respect to t and x,

$$\partial(E\cdot 1/2\cdot c_*\sin\theta)/\partial y+1/2\cdot E\partial U/\partial y\cdot\cos\theta\sin\theta=0. \tag{12}$$

On substitution from equations (7)$\sim$(9), the integral of equation (12) gives

$$E\cdot\sin\theta/(\sigma_0-bU)^2=\text{const.} \tag{13}$$

or, from equation (9),

$$E\cdot\sin 2\theta=\text{const.} \tag{14}$$

The relative amplification of the waves is therefore given by

$$H/H_0=(E/E_0)^{\frac{1}{2}}=(\sin 2\theta_0/\sin 2\theta)^{\frac{1}{2}}, \tag{15}$$

where H and H_0 are the wave heights in the regions of current and no current respectively.

2.2 Shallow-water wave refraction due to current

As seen from equation (8), the wave length becomes longer than that in the region of no current when the current is in the positive x-direction. Hence the situation in which the relative wave velocity is given by equation (6) may be limited. Here the relation between the relative wave velocity and the local wave number is assumed to be given by the shallow-water wave relation of small amplitude waves:

$$k\cdot c_*^2=g\cdot\tanh kh, \tag{16}$$

where h is the water depth. Equations (3) and (5) are applicable also in this case. In the same manner as in 2.1, we have

$$c_*/c_0=1/(1-U/c_0\cdot\cos\theta_0)\cdot\tanh kh/\tanh k_0h_0, \tag{17}$$
$$k/k_0=(1-U/c_0\cdot\cos\theta_0)^2\cdot\tanh k_0h_0/\tanh kh, \tag{18}$$
$$\cos\theta/\cos\theta_0=1/(1-U/c_0\cdot\cos\theta_0)^2\cdot\tanh kh/\tanh k_0h_0, \tag{19}$$

where h_0 is the water depth in the region of no current ($y<0$). It is evident that

in this case the terms underlined are added to equations (7)～(9) in the case of deep-water wave refraction. As seen from equation (18), the unknown k is included in both left and right hand sides. So it is necessary to calculate the value of k by iteration.

The relative group velocity is given by

$$c_{g*}/c_* = n_* = 1/2 \cdot (1 + 2kh/\sinh 2kh). \tag{20}$$

Using equation (20), equation (10) becomes in this case

$$\frac{\partial}{\partial y}\left(\frac{n_* \cdot E \cdot \tanh kh \cdot \sin\theta}{\sigma_0 - bU} \right) + \frac{n_* \cdot E \cdot b \cdot \tanh kh \cdot \sin\theta}{(\sigma_0 - bU)^2} \frac{\partial U}{\partial y} = 0. \tag{21}$$

The integral of equation (21) gives

$$n_* \cdot E \cdot \tanh kh \cdot \sin\theta / (\sigma_0 - bU)^2 = \text{const.}, \tag{22}$$

or, from equation (19),

$$n_* \cdot E \cdot \sin 2\theta = \text{const.} \tag{23}$$

The relative amplification of the waves is therefore given by

$$H/H_0 = (E/E_0)^{\frac{1}{2}} = (\sin 2\theta_0 / \sin 2\theta)^{\frac{1}{2}} \cdot (n_0/n_*)^{\frac{1}{2}}, \tag{24}$$

where n_0 is n in the region of no current.

Since $\cos\theta$ in equation (19) can not exceed unity, there is clearly an upper limit to U for which a solution exists:

$$U/c_0 \leq \{1 - (\cos\theta_0 \cdot \tanh kh/\tanh k_0h_0)^{\frac{1}{2}}\}/\cos\theta_0. \tag{25}$$

It is evident that in the case of deep-water wave refraction the term underlined in equation (25) is equal to unity. At this upper limit θ becomes equal to 0, and the waves are interrupted to proceed by the current. On the other hand, for negative current $U<0$, there is no kinematic limit to U. However, as $U \to -\infty$, k becomes very large, that is to say, the wave length becomes very small (Fig. 1, (b)). The angle θ approaches 90°, that is, the direction of propagation becomes nearly normal to the current. Fig. 2 shows the variations of the wave direction. The broken line curves are for the deep-water wave refraction (equation (9)). The full line curves are examples for the shallow-water wave refraction ($k_0h_0 = 0.1$ in equation (19)). It is evident that in the shallow-water wave refraction the wave direction varies more rapidly than in the deep-water wave refraction.

As seen from equations (15) and (24), the wave height becomes infinite both when $\theta \to 0°$ and $\theta \to 90°$. Longuet-Higgins and Stewart[1] described on this phenomenon as follows:

> In the first case the infinity is not significant: it is due to the fact that the ray-paths intersect, and the corresponding line y=const. is a caustic.

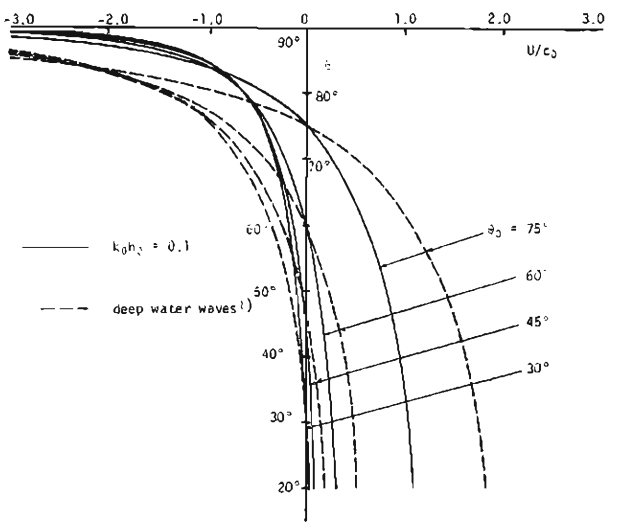

Fig. 2. Variation of direction of waves crossing a shearing current at an oblique angle θ for various initial angles θ_0

In the neighbourhood of such a line the ordinary approximations of ray optics do not apply; a higher-order theory, generally involving Airy functions, must be used. One may expect that the wave amplitude in fact remains finite even in the neighbourhood of the critical line.

The second case, when $\theta \to 90^{\circ}$, corresponds to the limit $U \to -\infty$. In that case the infinity is genuine and is due mainly to the fact that the wave length and wave velocity are so much reduced that, in order to maintain the

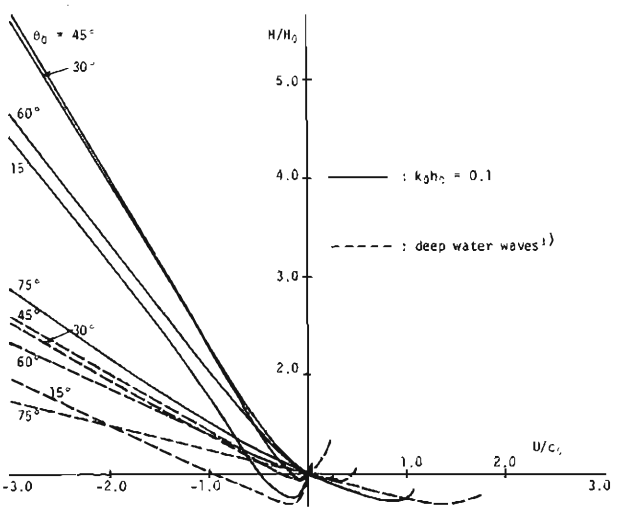

Fig. 3. Variation of height of waves crossing a shearing current at an oblique angle for various initial angles θ_0

energy flux in the y-direction, the wave height must increase. In practice the waves may break; but for no finite velocity $U<0$ is the ratio H/H_0 theoretically infinite.

We may note that it is possible for the component of stream velocity opposite to the waves to exceed the group velocity:

$$1/2 \cdot c_* + U \cos\theta < 0.$$

The waves are not thereby stopped, for the wave amplitude tends to be diminished by a lateral stretching of the wave crests.

Fig. 3 shows the variations of the wave height H. The broken line curves are for the deep-water wave refraction (equation (15)), and the full line curves are examples for the shallow-water wave refraction ($k_0h_0=0.1$ in equation (24)). It is evident that in the shallow-water wave refraction the wave height varies more rapidly than in the deep-water wave refraction.

2.3 Effect of radiation stress

Dividing equation (19) by equation (17) yields

$$\cos\theta/\cos\theta_0 = (c_*/c_0)/(1-U/c_0 \cdot \cos\theta_0). \tag{26}$$

Substituting equation (26), equation (24) becomes

$$H/H_0 = (n_0c_0/n_*c_*)^{\frac{1}{2}} \cdot (\sin\theta_0/\sin\theta)^{\frac{1}{2}} \cdot (1-U/c_0 \cdot \cos\theta_0)^{\frac{1}{2}}. \tag{27}$$

If the deep-water wave velocity without current c_d is used as c_0, $n_0=n_d=1/2$ and equation (27) becomes

$$H/H_d = K_s' \cdot K_r' \cdot K_{rs}, \tag{28}$$

$$K_s' = (c_d/2n_*c_*)^{\frac{1}{2}}, \tag{29}$$

$$K_r' = (\sin\theta_d/\sin\theta)^{\frac{1}{2}}, \tag{30}$$

$$K_{rs} = (1-U/c_d \cdot \cos\theta_d)^{\frac{1}{2}}. \tag{31}$$

The coefficient K_s' has the same form as the shoaling coefficient K_s except for that n and c are replaced with n_* and c_*. This coefficient means the rate of wave height variation due to not only the water depth variation but also the current. The coefficient K_r' has the same form as the refraction coefficient K_r. The wave direction θ is however the refracted wave direction not only by the underwater topography but also due to the current. If the radiation stress is neglected in equation (21), it will be found that

$$H/H_d = K_s' \cdot K_r'. \tag{32}$$

The coefficient K_{rs} therefore represents the effect of the radiation stress on the wave height variation. In equation (31), $\cos\theta_d$ is positive for $0°<\theta_d<90°$. Therefore if $U>0$, that is, the current is in the same direction of the waves, $K_{rs}<1$ so that the wave height is damped. On the contrary, if $U<0$, that is, the current is in the

opposite direction to the waves, $K_{rs}>1$ so that the wave height is amplified.

3. Numerical Model of Wave Refraction Due to Current

3.1 Wave orthogonal equation

In the theoretical treatment, the wave direction θ is determined with the irrotational condition of the wave number (equation (2)). On the other hand, in the conventional numerical technique for wave refraction by underwater topography[14], the wave direction is determined by the equation of the curvature of a ray along the ray. A similar equation is derived by Arthur[15] for the wave refraction due to current.

$$d\theta/dt=\partial(q_c+c_*)/\partial x\cdot\sin\theta-\partial(q_c+c_*)/\partial y\cdot\cos\theta, \tag{33}$$

$$dx/dt=U+c_*\cos\theta,\ dy/dt=V+c_*\sin\theta, \tag{34}$$

where x and y are the horizontal coordinates, U and V are x- and y- components of the current and q_c is the component of the current in the direction of c_* as shown in Fig. 4:

$$q_c=U\cos\theta+V\sin\theta. \tag{35}$$

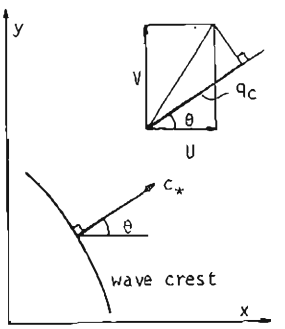

Fig. 4. Definition diagram for numerical model of wave refraction due to current.

The above equations mean that the variation of the wave direction θ with time along a path given by equation (34) is represented by equation (33). Skovgaard and Jonsson[12] called equation (33) "wave orthogonal equation".

A similar equation is also derived from the irrotational condition of wave number (equation (2)). Using the relationships $k_x=k\cos\theta$ and $k_y=k\sin\theta$, equation (2) is transformed as

$$\cos\theta\cdot\partial\theta/\partial x+\sin\theta\cdot\partial\theta/\partial y=\cos\theta/k\cdot\partial k/\partial y-\sin\theta/k\cdot\partial k/\partial x. \tag{36}$$

The kinematic conservation equation of waves (4) is given in this two-dimensional

case as

$$k(c_*+U\cos\theta+V\sin\theta)=\sigma_0. \tag{37}$$

Differentiating equation (37) yields

$$\frac{\partial k}{\partial x}=\frac{-\sigma_0\left\{\frac{\partial c_*}{\partial x}+\frac{\partial U}{\partial x}\cos\theta+\frac{\partial V}{\partial x}\sin\theta+\frac{\partial\theta}{\partial x}(-U\sin\theta+V\cos\theta)\right\}}{(c_*+U\cos\theta+V\sin\theta)^2} \tag{38}$$

and

$$\frac{\partial k}{\partial y}=\frac{-\sigma_0\left\{\frac{\partial c_*}{\partial y}+\frac{\partial U}{\partial y}\cos\theta+\frac{\partial V}{\partial y}\sin\theta+\frac{\partial\theta}{\partial y}(-U\sin\theta+V\cos\theta)\right\}}{(c_*+U\cos\theta+V\sin\theta)^2}. \tag{39}$$

Substituting equations (37)～(39), equation (36) becomes

$$\begin{aligned}&\frac{\partial\theta}{\partial x}(U+c_*\cos\theta)+\frac{\partial\theta}{\partial y}(V+c_*\sin\theta)\\&=\left(-\frac{\partial U}{\partial y}\cos\theta+\frac{\partial U}{\partial x}\sin\theta\right)\cos\theta+\left(-\frac{\partial V}{\partial y}\cos\theta+\frac{\partial V}{\partial x}\sin\theta\right)\sin\theta\\&+\left(-\frac{\partial c_*}{\partial y}\cos\theta+\frac{\partial c_*}{\partial x}\sin\theta\right).\end{aligned} \tag{40}$$

The rate of variation with time along the path given by equation (34) is written as

$$\frac{d}{dt}=\frac{\partial}{\partial t}+\frac{dx}{dt}\frac{\partial}{\partial x}+\frac{dy}{dt}\frac{\partial}{\partial y}=(U+c_*\cos\theta)\frac{\partial}{\partial x}+(V+c_*\sin\theta)\frac{\partial}{\partial y} \tag{41}$$

in the steady state. Equation (40) is therefore expressed as follows:

$$\begin{aligned}\frac{d\theta}{dt}&=\left(-\frac{\partial U}{\partial y}\cos\theta+\frac{\partial U}{\partial x}\sin\theta\right)\cos\theta+\left(-\frac{\partial V}{\partial y}\cos\theta+\frac{\partial V}{\partial x}\sin\theta\right)\sin\theta\\&+\left(-\frac{\partial c_*}{\partial y}\cos\theta+\frac{\partial c_*}{\partial x}\sin\theta\right).\end{aligned} \tag{42}$$

On the other hand, equation (33), substituting equation (35), becomes

$$\begin{aligned}\frac{d\theta}{dt}&=\left(-\frac{\partial U}{\partial y}\cos\theta+\frac{\partial U}{\partial x}\sin\theta\right)\cos\theta+\left(-\frac{\partial V}{\partial y}\cos\theta+\frac{\partial V}{\partial x}\sin\theta\right)\sin\theta\\&+\left(-U\sin^2\theta+V\sin\theta\cdot\cos\theta\right)\frac{\partial\theta}{\partial x}+\left(-V\cos^2\theta+U\sin\theta\cdot\cos\theta\right)\frac{\partial\theta}{\partial y}\\&+\left(-\frac{\partial c_*}{\partial y}\cos\theta+\frac{\partial c_*}{\partial x}\sin\theta\right).\end{aligned} \tag{43}$$

It is evident that equation (43) has the additional terms containing $\partial\theta/\partial x$ and $\partial\theta/\partial y$ compared with equation (42). This discrepancy is not discussed here. Equations (42) and (34) derived from the irrotational condition of wave number are used in this numerical model.

Noda et al.[11] used equation (36) giving the irrotational condition of wave number, but they solved equation (36) directly on the numerical grid points instead of using the technique of integrating along the path given by equation (34).

3.2 Relative wave velocity to current

As mentioned above, the kinematic conservation equation of waves in current is represented as follows:

$$k(c_*+U\cos\theta+V\sin\theta)=\sigma_0=2\pi/T, \tag{44}$$

where T is the period of waves in the region of no current. On the other hand, equation (16) is assumed as the relation between the relative wave velocity to current and the local wave number. Combining equations (44) and (16), we have

$$L_*\equiv\frac{2\pi}{k}=\frac{gT^2/2\pi\cdot\tanh(2\pi h/L_*)}{(1-T/L_*\cdot U\cos\theta-T/L_*\cdot V\sin\theta)^2}. \tag{45}$$

Therefore if the wave period T, the water depth h, two components of current velocity U and V and the wave direction θ are known, the wave length L_* is determined by iteration. Then the relative wave velocity c_* is obtained from equation (16). The characteristics of the wave length in current was discussed in detail by Jonsson, Skovgaard and Wang[18].

3.3 Wave energy equation

The wave energy conservation equation in current (10) derived by Longuet-Higgins and Stewart[1] is used here. Considering the steady state and the representation of the radiation stress (11), equation (10) becomes

$$(U+c_{g*}\cos\theta)\frac{\partial E}{\partial x}+(V+c_{g*}\sin\theta)\frac{\partial E}{\partial y}=F(U,V,c_*,c_{g*},\theta)\cdot E, \tag{46}$$

where

$$\begin{aligned}F=&-\frac{\partial U}{\partial x}+\frac{\partial V}{\partial y}+-\frac{\partial c_{g*}}{\partial x}\cos\theta+\frac{\partial c_{g*}}{\partial y}\sin\theta+c_{g*}\left(-\sin\theta\frac{\partial\theta}{\partial x}+\cos\theta\frac{\partial\theta}{\partial y}\right)\\&+\left\{\frac{c_{g*}}{c_*}\cos^2\theta+\frac{1}{2}\left(\frac{2c_{g*}}{c_*}-1\right)\right\}\frac{\partial U}{\partial x}+\frac{c_{g*}}{c_*}\cos\theta\cdot\sin\theta\left(\frac{\partial V}{\partial x}+\frac{\partial U}{\partial y}\right)\\&+\left\{\frac{c_{g*}}{c_*}\sin^2\theta+\frac{1}{2}\left(\frac{2c_{g*}}{c_*}-1\right)\right\}\frac{\partial V}{\partial y}.\end{aligned} \tag{47}$$

Lets consider a path given by

$$dx/dt=U+c_{g*}\cos\theta,\quad dy/dt=V+c_{g*}\sin\theta. \tag{48}$$

Along this path, the rate of wave energy variation with time is, from equation (46), given as

$$dE/dt=F(U,V,c_*,c_{g*},\theta)\cdot E. \tag{49}$$

This representation of the wave energy variation is similar to that of the wave direction variation (42) and (34). Two paths given by equations (34) and (48) do not coincide, for c_{g*} is not equal to c_* in general. Furthermore, the term F contains the wave direction θ. So, before the calculation of the wave energy variation, it is necessary to calculate the wave direction variation by using equations (42) and (34).

In the conventional numerical technique of wave refraction by underwater topography[4], the refraction coefficient is calculated at each step point along a ray according to the theory developed by Munk and Arthur[7]. It is clear that the calculation of the wave height in wave refraction due to current is not so simple compared with the calculation in wave refraction by underwater topography only.

Noda et al. solved equation (46) directly on the numerical grid points. In this numerical model, equations (48) and (49) are used. The wave height H is calculated with the relationship $E=1/8\cdot\rho gH^2$.

3.4 Numerical computation

The region of computation is constructed by a set of perpendicular grids of equal spacing Δs (Fig. 5). At each grid point, the water depth h, two components of current velocity U and V are known. On the offshore boundary $j=1$, the initial wave direction θ_0 and the initial wave height H_0 are known. The wave period T is given and constant in the whole region. The numerical computation consists of two parts. In the first part, the wave direction θ is calculated by using equations (42) and (34). After that, the wave height H is calculated by using the calculated values of wave direction and the equations (48) and (49).

The path in the calculation of wave direction given by equation (34) starts at each grid point on the offshore boundary $j=1$. Along each path, the new step point (x_m, y_m) and the wave direction θ_m are calculated every time increment Δt (Fig. 6). In practice, at each step, the temporary increment of θ (denoted by $\Delta\theta_m'$) is calculated

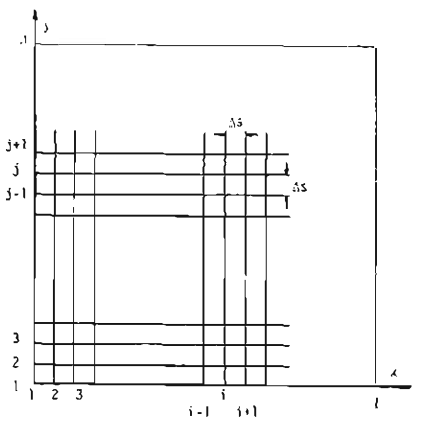

Fig. 5. Set of perpendicular grids of equal spacing Δs.

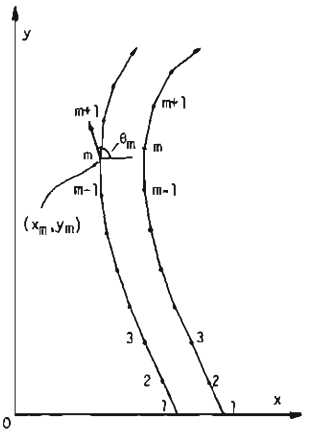

Fig. 6. Paths in calculation of wave direction.

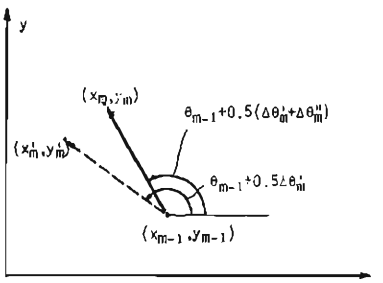

Fig. 7. Temporary step point.

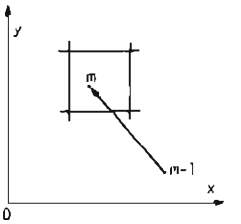

Fig. 8 Interpolation from values on four grid points surrounding a step point

at first (Fig. 7). The temporary step point (x_m', y_m') is calculated by the equations

$$x_m' = x_{m-1} + c_{*m-1} \cdot \cos(\theta_{m-1} + 1/2 \cdot \Delta\theta_m') \cdot \Delta t + U_{m-1} \cdot \Delta t, \tag{50}$$

$$y_m' = y_{m-1} + c_{*m-1} \cdot \sin(\theta_{m-1} + 1/2 \cdot \Delta\theta_m') \cdot \Delta t + V_{m-1} \cdot \Delta t. \tag{51}$$

At this temporary point, the increment of θ (denoted by $\Delta\theta_m''$) is calculated again. The final new wave direction and the new step point are calculated by the equations

$$\theta_m = \theta_{m-1} + 1/2 \cdot (\Delta\theta_m' + \Delta\theta_m''), \tag{52}$$

$$x_m = x_{m-1} + c_{*m-1} \cdot \cos\theta_m \cdot \Delta t + U_{m-1} \cdot \Delta t, \tag{53}$$

$$y_m = y_{m-1} + c_{*m-1} \cdot \sin\theta_m \cdot \Delta t + V_{m-1} \cdot \Delta t. \tag{54}$$

In general, the step point does not coincide with the grid point (Fig. 8). In the calculation of equations (42) and (34), the interpolated value from the values on four grid points surrounding the step point is used. The derivatives of U, V and c_* with respect to x and y are also calculated from the values on four grid points.

The calculation of wave direction along each path is stopped if the path runs out of the boundary of the computation region. Therefore, in general, some part of the computation region is left in which the value of wave direction is not calculated

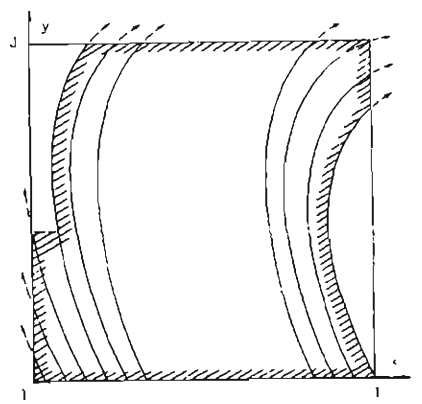

Fig. 9. Region in which wave directions are calculated.

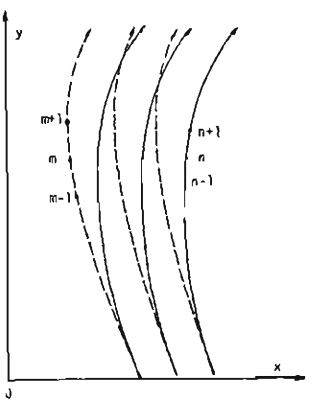

Fig. 10. Paths in calculation of wave height.

(Fig. 9). The values of θ on the grid points are interpolated from the calculated values of θ on the nearest three step points for the next calculation of wave height.

The path in the calculation of wave height given by equation (48) also starts at each grid point on the offshore boundary $j=1$. Along each path, the new step point (x_n, y_n) and new wave height H_n are calculated every time increment Δt by using equation (49) (Fig. 10). In the wave height calculation, the temporary step point used in the wave direction calculation is not used. In the same manner as in the wave direction calculation, the values and derivatives at the step point are interpolated from the values on four grid points surrounding the step point. The calculation of wave height along each path is stopped if the path runs out of the region where the interpolated values of wave direction are registered on the grid points.

As an example of the numerical computation, a 500 m×500 m rectangular region with a simple current of only the x-component of velocity U increasing linearly in the y-direction (Fig. 11) is considered.

$$U=\begin{cases}0 : 0\leq y\leq 80 \text{ m},\\ 0.01(y-80) \text{ m/s} : 80 \text{ m}\leq y\leq 500 \text{ m}.\end{cases} \tag{55}$$

The cases of constant water depth and plane beach are considered. In the case of plane beach the water depth decreases in the y-direction and becomes 0 at $y=500$ m. The grid spacing Δs is set equal to 20 m, and the wave period T is 5 sec. The time increment Δt is set equal to $1/2 \cdot T$. In the numerical model, the current U takes only positive value, and the wave direction θ can vary from 0° to 180°. The numerical results for $\theta_0>90°$ are comparable with the theoretical results for the initial wave direction of $\theta_0-90°$ and the current $-U$. The initial wave height H_0 is 1m.

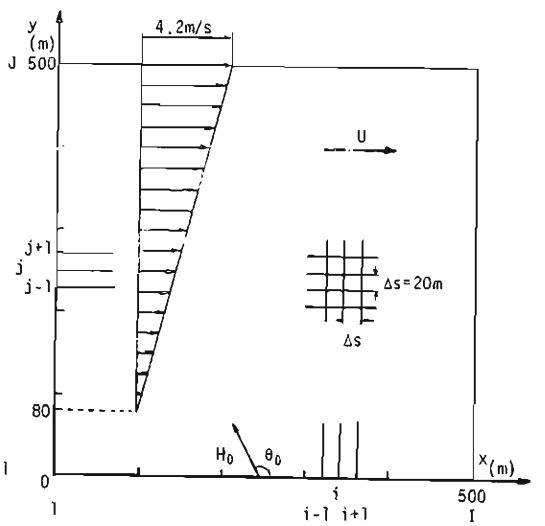

Fig. 11. 500m×500m rectangular region with a simple current of only x-component of velocity U increasing linearly in y-direction.

4. Results of Numerical Computation and Discussions

4.1 Comparisons of numerical and theoretical results

Fig 12 shows an example of comparisons of the numerical and theoretical results for the cases of plane beach without current. In this case, the slope of beach is 1/50. At the offshore boundary $y=0$ the water depth is 10 m and the initial wave direction θ_0 is 135° (Fig. 11). The theoretical values are calculated by using equations (19) and (24). The numerical results agree well with the theoretical results, and they show the well known behaviours that the wave direction becomes normal to the beach and the wave height decreases at first and increases as the waves approach the shoreline.

Fig. 13 shows the result of the case of uniform depth $h=30$m and the current given by equation (55). The initial direction of waves θ_0 is 60°, and the current is in the same direction of the waves. The numerical and theoretical results agree roughly. The wave direction becomes parallel to the direction of current gradually and the wave height decreases with increase in y. The theoretical curve of wave height increases after the initial decrease. This increase is not significant as described in the theoretical treatment. The numerical result does not exist in the range of the theoretical increase of wave height, because all paths run out of the boundary of computation region before approaching the boundary $y=500$m.

Fig. 14 shows the result of the same case as in Fig. 13 except for $\theta_0=120°$. The current is in the opposite direction to the waves. The numerical and theoretical results agree roughly also in this case. The wave direction becomes normal to the direction of the current gradually and the wave height increases with increase in y.

Fig. 15 shows the result of the same case as in Fig. 14 except for the uniform water depth $h=10$m. The numerical and theoretical results agree roughly. Compared

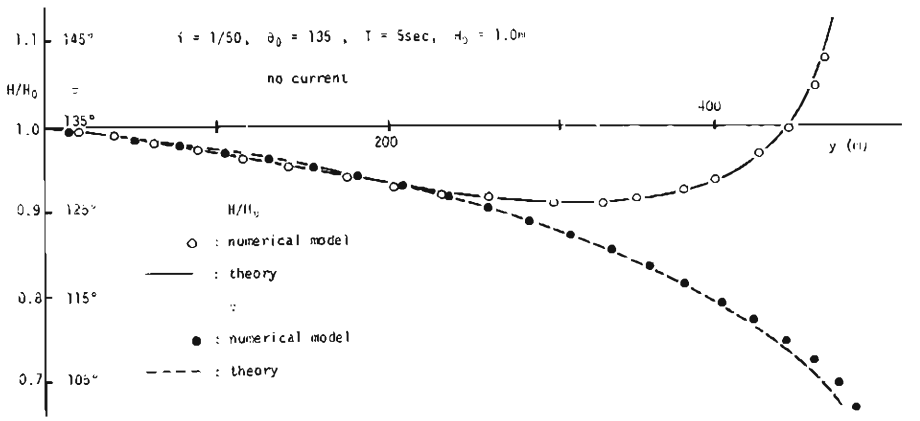

Fig. 12. Comparison between numerical and theoretical results for case of plane beach without current (beach slope=1/50, $\theta_0=135°$).

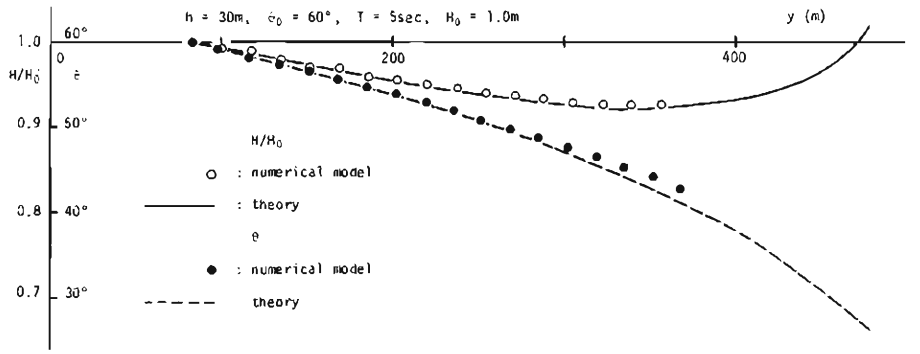

Fig. 13. Comparison between numerical and theoretical results for case of uniform depth ($h=30$ m, $\theta_0=60°$).

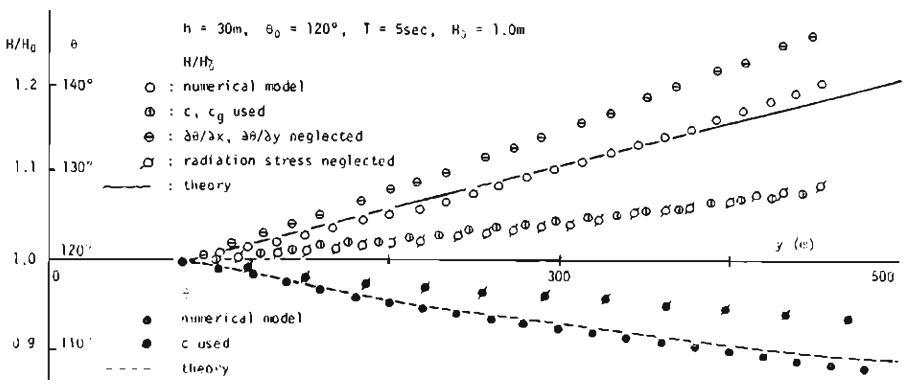

Fig. 14. Comparison between numerical and theoretical results for case of uniform depth ($h=30$ m, $\theta_0=120°$).

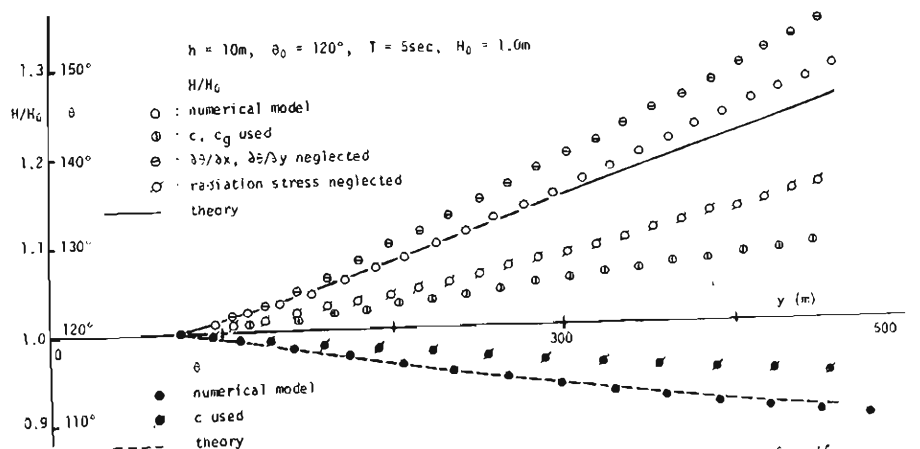

Fig. 15. Comparison between numerical and theoretical results for case of uniform depth ($h=10$ m, $\theta_0=120°$).

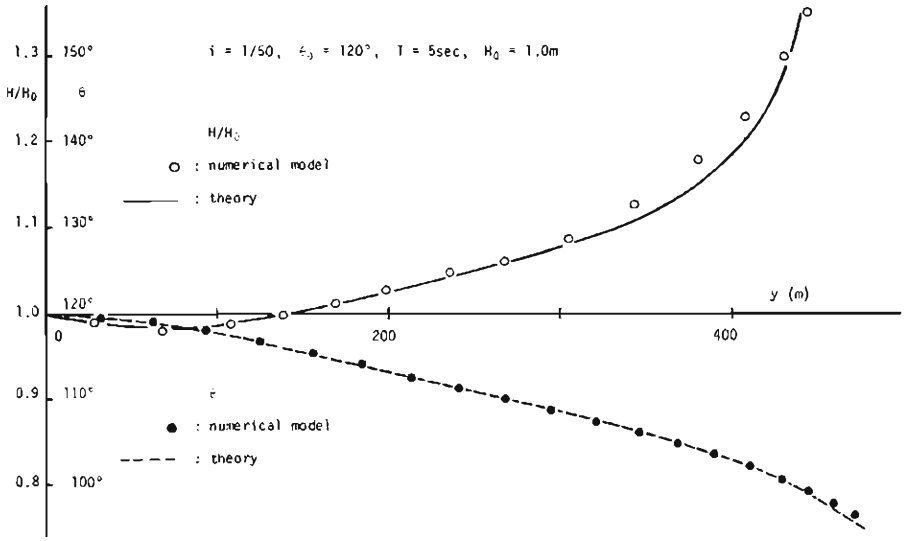

Fig. 16. Comparison between numerical and theoretical results for case of plane beach (beach slope=1/50, $\theta_0=120°$).

with Fig. 14, the variations of wave direction and wave height for $h=10$ m resemble the variations for $h=30$ m. The rate of increase of wave height for $h=10$ m is however larger than that for $h=30$m. Also the differences between the numerical and theoretical results of wave height for $h=10$m are larger than those for $h=30$ m.

Fig. 16 shows an example of the results of the cases of plane beach and current. The slope of beach is 1/50 which is the same as the case of no current (Fig. 12). The initial wave direction is 120°. The numerical and theoretical results also agree roughly. As well as the case of Fig. 12, the wave direction becomes normal to the direction of the current gradually due to the underwater topography and the opposite current. The wave height becomes larger than that in the case of Fig. 12, because the rate of wave height increase is amplified by the opposite current.

As seen from five examples in Figs. 12~16, the numerical results agree roughly with the theoretical results. The differences between them however increase with increase in y. This is because the errors at each step in the numerical computation accumulate as the paths go on in the region of computation.

4.2 Effects of c_* and c_{g*}, $\partial\theta/\partial x$ and $\partial\theta/\partial y$ and radiation stress

As seen from equation (45), the wave length in the presence of current L_* is not equal to the wave length of small amplitude waves in the absence of current L. The relative wave velocity to the current c_* and the relative group velocity to the current c_{g*} calculated by using equations (16) and (20) respectively are also not equal to c and c_g in the absence of current. The value of wave direction θ is necessary to be known before the calculation of the wave length L_* by using equation (45). And the wave direction θ is one of the unknowns to be determined by

the numerical computation. This is one of the reasons why the numerical computation of wave refraction due to current is complicated compared with the numerical computation of wave refraction by underwater topography. If it would be possible to use c and c_g instead of c_* and c_{g*}, the computation would become fairly simple. In Figs. 14 and 15, two examples of the comparisons between the numerical results using c, c_g and c_*, c_{g*} under the same conditions are shown. In these cases, the calculated values of wave direction by using c are about the half of the value by using c_*, and the values of wave height by using c and c_g are about 30% or 40% of the values by using c_* and c_{g*}. As seen from these examples, the relative wave velocity and group velocity to current c_* and c_{g*} have to be used in the computation of wave refraction due to current.

As mentioned in **3**, there are two kinds of wave orthogonal equations, (42) and (43). In this numerical model, equation (42) is used. The effects of the terms containing $\partial\theta/\partial x$ and $\partial\theta/\partial y$ in equation (43) are therefore not discussed. On the other hand, the term F in the equation of wave energy variation (49) also has a term containing $\partial\theta/\partial x$ and $\partial\theta/\partial y$ (equation (47)) :

$$c_{g*}(-\sin\theta\cdot\partial\theta/\partial x+\cos\theta\cdot\partial\theta/\partial y).$$

In Figs. 14 and 15, two examples of comparisons between the numerical results of wave height considering and neglecting the term containing $\partial\theta/\partial x$ and $\partial\theta/\partial y$ in F are shown. In these cases, the values neglecting the term are about 1.2 times as large as the values considering the term. The term containing $\partial\theta/\partial x$ and $\partial\theta/\partial y$ in F is therefore not negligible in the computation of wave height.

Finally, the effect of the radiation stress on the wave height variation is discussed. The last three terms in F

$$\begin{aligned}&\{c_{g*}/c_*\cdot\cos^2\theta+1/2\cdot(2c_{g*}/c_*-1)\}\cdot\partial U/\partial x\\&+c_{g*}/c_*\cdot\cos\theta\cdot\sin\theta(\partial V/\partial x+\partial U/\partial y)\\&+\{c_{g*}/c_*\cdot\sin^2\theta+1/2\cdot(2c_{g*}/c_*-1)\}\cdot\partial V/\partial y\end{aligned}$$

represent the effect of the radiation stress. In Figs. 14 and 15, two examples of comparisons between the results of wave height considering and neglecting those terms are shown. The calculated values of wave height neglecting those terms are about a half of the values considering the radiation stress. The effect of the radiation stress is therefore not negligible in the computation of wave height.

As described above, any of the effects of c_* and c_{g*}, $\partial\theta/\partial x$ and $\partial\theta/\partial y$ and the radiation stress is not negligible at least in the cases treated here. These discussions are however limited to the cases treated here. It is necessary to apply this numerical model to many cases of currents of various distributions for the discussion of general characteristics of these effects.

5. Conclusions

The wave refraction and the wave height variation due to current are discussed by

a theoretical treatment and a numerical model. The main conclusions are as follows:

1) The theory of refraction of deep-water waves traversing a simple horizontal current with vertical axis of shear by Longuet-Higgins and Stewart[1] is extended to the case of shallow-water waves. The wave direction and wave height of shallow-water waves refracted by the current vary more rapidly than those of deep-water waves.
2) The variation of wave height in this case is expressed as the product of the similar coefficients to the well known shoaling and refraction coefficients and a coefficient representing the effect of radiation stress.
3) The wave orthogonal equation for wave refraction due to current given by Arthur[15] has additional terms containing the derivatives of wave direction with respect to the horizontal coordinates compared with the equation derived from the irrotational condition of wave number.
4) A numerical model is presented for the wave refraction due to current. The effect of the waves on the current is neglected in this model. This model consists of two parts: the computation of wave direction and the computation of wave height. The variation of wave direction is calculated with the wave orthogonal equation derived from the irrotational condition of wave number, which represents the variation of wave direction with time along a path propagating in the direction of the sum of the wave velocity and the current. The variation of wave height is also calculated with the equation of wave energy conservation in current derived by Longuet-Higgins and Stewart[1], along another path propagating in the direction of the sum of the group velocity and the current.
5) The numerical results agree roughly with the theoretical results, and the validity of the numerical model is roughly confirmed
6) The effect of the relative wave velocity to the current is not negligible in the computation of wave refraction due to current. Also the effects of the derivatives of wave direction with respect to the horizontal coordinates and the radiation stress on the wave height variation are not negligible.

A part of the present investigation was accomplished with the support of the Science Research Fund of the Ministry of Education for which the authors express their appreciation.

References

1) Longuet-Higgins, M. S. and R. W. Stewart: The changes in amplitude of short gravity waves on steady non-uniform currents, Jour. Fluid Mech., Vol. 10, 1961, pp. 529-549.
2) Unna, P. J. H.: Waves and tidal streams, Nature, Lond., Vol. 149, 1942, pp. 219-220.
3) Johnson, J. W.: The refraction of surface waves by currents, Trans. Amer. Geophys. Union, Vol. 28, 1947, pp. 867-874.
4) Evans, J. T.: Pneumatic and similar breakwater, Proc. Roy. Soc., A. 231, 1955, pp. 457-466.
5) Bowen, A. J.: The generation of longshore currents on a plane beach, Jour. Marine Res., Vol. 27, No. 2, 1969, pp. 206-215.

6) Thornton, E. B.: Variation of longshore current across the surf zone, Proc. 12th Conf. Coastal Eng., 1970, pp. 291-308.
7) Longuet-Higgins, M. S.: Longshore currents generated by obliquely incident sea waves, Parts 1 and 2, Jour Geophys. Res., Vol. 75, No. 33, 1970, pp. 6778-6801.
8) Arthur, R. S.: A note on the dynamics of rip currents, Jour. Geophys. Res., Vol. 67, No. 7, 1962, pp. 2777-2779.
9) Bowen, A. J.: Rip currents, Part 1, Theoretical investigations, Jour. Geophys. Res., Vol. 74, No. 23, 1969, pp. 5467-5478.
10) Bowen, A. J. and D. L. Inman: Rip currents, Part 2, Laboratory and field observations, Jour. Geophys. Res., Vo. 74, No. 23, 1969, pp. 5478-5490.
11) Noda, E. K., C. J. Sonu, V. C. Rupert and J. I. Collins: Nearshore circulations under sea breeze conditions and wave-current interactions in the surf zone, Tetra Tech. Rep. TC-P-72-149-4, AD 776643, 1974.
12) Skovgaard, O. and I. G. Jonsson: Current depth refraction using finite elements, Proc. 15th Conf. Coastal Eng., 1976, pp. 721-737.
13) Phillips, O. M.: The Dynamics of the Upper Ocean, Cambridge University Press, 1966, pp. 43-44.
14) Griswold, G. M.: Numerical calculation of wave refraction, Jour. Geophys. Res., Vol. 63, No. 6, 1963, pp. 1715-1723.
15) Arthur, R. S.: Refraction of shallow water waves: The combined effect of currents and underwater topography, Trans. Amer. Geophys. Union, Vol. 31, No. 4, 1950, pp. 549-552.
16) Jonsson, I. G., O. Skovgaard and J. D. Wang: Interaction between waves and currents, Proc. 12th Conf. Coastal Eng., 1970, pp. 489-507.
17) Munk, W. H. and R. S. Arthur: Wave intensity along a refracted ray, National Bureau of Standard, Circ. 521, Gravity Waves, 1952.